Available online at www.sciencedirect.com
ScienceDirect
Journal of Photochemistry and Photobiology A: Chemistry 192 (2007) 23–28
Journal of Photochemistry and Photobiology A:Chemistry
www.elsevier.com/locate/jphotochem

Spectroscopic investigation of the interaction between rifabutin and bovine serum albumin

Cong-Xia Wang, Fang-Fei Yan, Yi-Xuan Zhang, Ling Ye *

School of Chemical Biology and Pharmaceutical Sciences, Capital Medical University, Beijing 100069, PR China

Received 22 February 2007; received in revised form 28 March 2007; accepted 30 April 2007
Available online 3 May 2007

Abstract

The binding of rifabutin (RB) to bovine serum albumin (BSA) was investigated by fluorescence spectroscopy and circular dichroism (CD). RB effectively quenched the intrinsic fluorescence of BSA via a combination of static and dynamic quenching. The thermodynamic parameters, ΔH° and ΔS° were estimated to be $-5.14\,\mathrm{kJ\,mol^{-1}}$, $+120.44\,\mathrm{J\,mol^{-1}\,K^{-1}}$ according to the van't Hoff equation. This indicates that hydrophobic interaction plays a major role in stabilizing the RB–BSA complex. The high order of magnitude of k_q (10^{15}) for RB–BSA suggests that the process of energy transfer occurs through intermolecular interaction. Binding studies in the presence of fluorescence probe, 8-anilino-1-naphthalein-sulphonic acid (ANS), showed that RB competed with ANS for hydrophobic sites on the surface of BSA. The effect of metal ion on the binding constant of RB–BSA complex varied with metal ion. Cu^{2+} and Ca^{2+} increased the binding constant, whereas Zn^{2+} and Mg^{2+} decreased the binding efficacy of RB to BSA. Synchronous fluorescence spectra and CD data revealed that RB induced the conformational change of BSA.

Keywords: Rifabutin (RB); Bovine serum albumin (BSA); Fluorescence quenching; Synchronous fluorescence; Circular dichroism (CD)

1. Introduction

Serum albumins are one of the most abundant proteins in blood plasma. Many drugs are transported in the blood upon binding to albumin. The binding ability of drug–albumin in blood stream may have a significant impact on distribution, free concentration, and metabolism of drug [1,2]. Thus, it is important and necessary to study the interaction of drug with serum albumins at molecular level [3–6].

Rifabutin (RB) (Scheme 1) is a potent semisynthetic spiropiperidyl-rifamycin derivative. It possesses a broad spectrum of antibacterial activity and is particularly active against mycobacterium tuberculosis, including rifampicin-resistant strains, and atypical mycobacteria. The antimicrobial action of the RB results from the inhibition of bacterial DNA-dependent RNA polymerase. Prophylactic treatment with RB was shown to decrease the incidence of mycobacterium avium complex (MAC) by approximately 50% in patients infected with human immunodeficiency virus. RB exhibits lower toxicity and have a longer half-life than rifampicin [7,8]. Previous studies suggested that protein binding of rifamycin antibacterials, e.g. rifampicin, rifabutin and rifapentine, may be a key parameter in their pharmacodynamics [9]. However, the binding mode and binding mechanism of RB with albumin are not clear so far. Thus, the interaction of RB with albumin needs to be investigated to provide binding parameters which are useful in studying the pharmacological response and design of dosage forms of RB.

Spectroscopic method has been widely applied in investigating drug binding with albumin under physiological conditions because of its accuracy, sensitivity, rapidity and convenience of usage [10–12]. It can reveal the accessibility of drugs to albumin's fluorophores, help understand the binding mechanisms of albumin-drug and provide information of the structural features that determine the therapeutic effectiveness of drug.

In this study, the interaction of RB with bovine serum albumin (BSA) was investigated via spectroscopic method. Fluorescence spectroscopy was employed to understand the quenching mechanism of RB–BSA binding as well as the impacts of common metal ions on RB–BSA interaction. Furthermore, binding of RB with BSA in the presence of fluorescence probe, 8-anilino-1-naphthalein-sulphonic acid (ANS), was conducted. Effects of RB on conformational changes of BSA were investigated by

* Corresponding author. Tel.: +86 10 83911525.
E-mail address: lingye@ccmu.edu.cn (L. Ye).

1010-6030/$ – see front matter © 2007 Elsevier B.V. All rights reserved.
doi:10.1016/j.jphotochem.2007.04.032

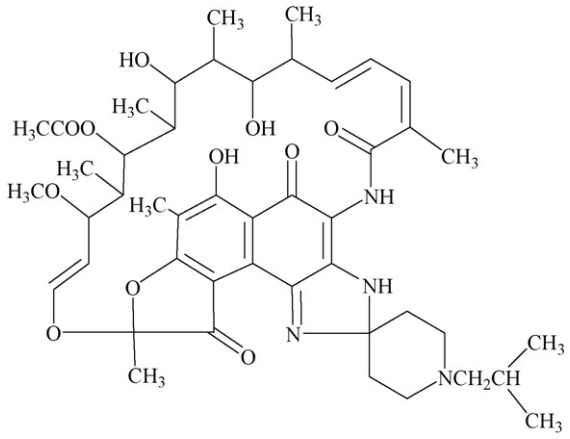

Scheme 1. The structure of rifabutin (RB).

synchronous fluorescence spectroscopy and circular dichroism (CD).

2. Materials and methods

2.1. Chemicals

Essentially-fatty-acid-free bovine serum albumin (BSA, fraction V) and 8-anilino-1-naphthalein-sulphonic acid sodium salt (ANS) were purchased from Sigma (USA). RB was obtained from Chengdu Yuyang Co., Ltd. (Sichuan, China). All other chemicals were of analytical grade and used as received.

2.2. Apparatus

Fluorescence emission spectra and synchronous spectra were collected on a RF-5301PC spetrofluorophotometer (Shimadzu, Japan) equipped with a SB-11 water bath (Eyela) and 1.0 cm quartz cells. The absorption spectra were recorded on a UV-2250 UV–vis spectrophotometer (Shimadzu, Japan). The CD measurements were performed on a JASCO-J-810 spectropolarimeter (JASCO, Japan) using a 0.1 cm quartz cell.

2.3. Procedures

Ten micromolar BSA solutions, based on their molecular weights of 68,000, were prepared by dissolving BSA in 0.1 M pH 7.4 phosphate buffer solution (PBS) containing 0.15 M NaCl. The stock solution of RB was prepared by dissolving its crystal in methanol/water (3:7) with final concentration of 0.45×10^{-3} M. Metal ions of 1×10^{-3} M were prepared in doubly distilled water.

In a typical fluorescence measurement, 2.0 mL 10 μM BSA was added to a 1.0 cm quartz cell. The RB solution was then gradually titrated to the cell using a micropipette. The concentrations of RB were ranged from 2.25 to 22.50 μM and the total accumulated volume of RB was less than 100 μL. The corresponding fluorescence emission spectra were recorded in the absence and presence of various metal ions from 300 to 500 nm upon excitation wavelength at 295 nm using 3/3 nm slit widths. All experiments were conducted at three temperatures, 298, 304, and 310 K as maintained by water bath. Synchronous fluorescence spectra of BSA titrated with various concentrations of RB were recorded from 300 to 400nm ($\Delta\lambda = 60$ nm) and from 280 to 350 nm ($\Delta\lambda = 15$ nm) with the excitation and emission slit widths of 3/1.5 nm, respectively. The UV–vis absorbance spectra of RB at 10 μM concentration was recorded at 298 K. CD spectra were recorded from 200 to 280 nm at 0.2 nm intervals with five scans averaged for each CD spectrum. The molar ratio of BSA to RB was varied as 1:0, 1:1 and 1:3.

Binding studies of RB and BSA in the presence of a fluorescence probe ANS were performed at two sets of experiments. (1) The interaction of RB/ANS with BSA was studied. BSA concentration was kept at 10 μM, whereas RB/ANS concentrations were at a variety of levels, from 2.25 to 22.5 μM, respectively. Fluorescence spectra of BSA were recorded from 300 to 500nm upon excitation at 295 nm. (2) The interaction of BSA–ANS in the presence of various concentrations of RB was investigated. The concentrations of BSA and ANS were 10 and 20 μM, respectively. RB was then gradually added to the BSA–ANS mixture. Fluorescence spectra of ANS were recorded in range of 390–550 nm upon excitation at 370 nm.

3. Results and discussion

3.1. Fluorescence studies of BSA quenched by RB

The interaction of RB with BSA was evaluated by monitoring the intrinsic fluorescence intensity changes of BSA upon addition of RB. Fluorescence quenching spectra of BSA at the presence of various concentrations of RB are shown in Fig. 1.

As illustrated in Fig. 1, the addition of RB led to a concentration-dependent quenching of BSA intrinsic fluorescence intensity along with a slightly red shift of maximum emission wavelength, implying that the binding of RB to BSA occurs and the microenvironment around chromophore of BSA is changed upon addition of RB.

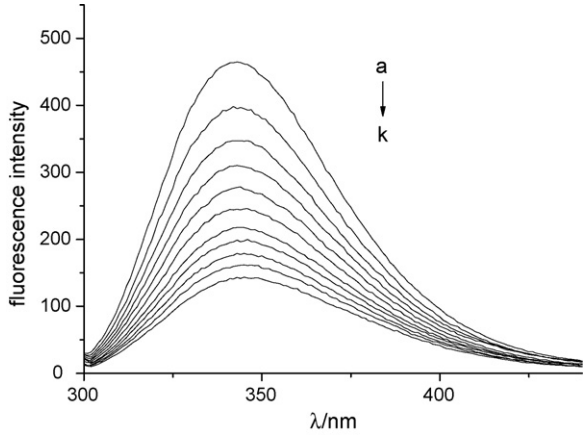

Fig. 1. Fluorescence quenching spectra of BSA at different concentrations of RB at 298 K; $C_{BSA} = 10$ μM; C_{RB} from (a) to (k): 0 μM (a), 2.25 μM (b), 4.5 μM (c), 6.75 μM (d), 9 μM (e), 11.25 μM (f), 13.5 μM (g), 15.75 μM (h), 18 μM (i), 20.25 μM (j), and 22.5 μM (k). $\lambda_{ex} = 295$ nm.

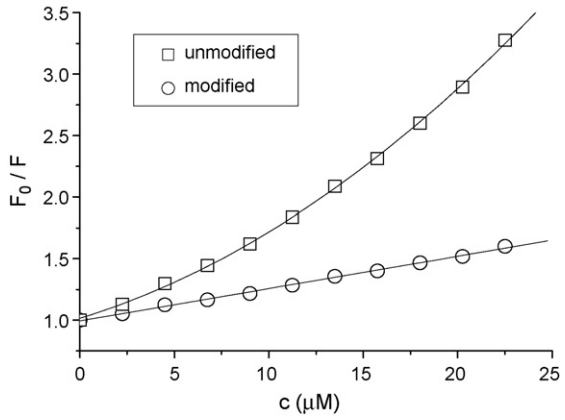

Fig. 2. Stern–Volmer and modified Stern–Volmer plots of RB interaction with BSA at 298 K; $C_{BSA} = 10\ \mu M$; $\lambda_{ex} = 295$ nm.

Fluorescence intensity data was then analyzed according to Stern–Volmer quenching equation [13]:

$$\frac{F_0}{F} = 1 + K_{sv}[Q] \tag{1}$$

where F_0 and F are the steady state fluorescence intensities of BSA at 343 nm before and after the addition of quencher (RB). K_{sv} and $[Q]$ are the Stern–Volmer dynamic quenching constant and the concentration of quencher RB, respectively.

Stern–Volmer plot of BSA with RB at 298 K is shown in Fig. 2. The plot shows a positive deviation (concave towards the y axis), suggesting the presence of a combination of static and dynamic quenching by the same fluorophore. According to Eftink and Ghiron [14,15], the upward curvature in the Stern–Volmer plot indicates that both tryptophan residues of BSA are exposed to the quencher. Accordingly, a modified Stern–Volmer equation that describes quenching data for both dynamic and as static quenching was applied [14]:

$$\frac{F_0}{F} = 1 + K_{sv}[Q]\exp(V[Q]) \tag{2}$$

where V is the static quenching constant and the value of V can be obtained from Eq. (2) by plotting $F_0/F\exp(V[Q]) - 1$ versus $[Q]$ for varying V until a linear plot is acquired. The K_{sv} can be then obtained from slope of $F_0/F\exp(V[Q]) - 1$ versus $[Q]$ plot. Values of V and K_{sv} at three different temperatures (298, 304 and 310 K) are consequently presented in Table 1.

As for a bimolecular quenching process, Eq. (3) is employed for the evaluation of the quenching rate constant k_q:

$$k_q = \frac{K_{sv}}{\tau_0} \tag{3}$$

where τ_0 is the average lifetime of biomolecules in the absence of quencher and the typical value of τ_0 for tryptophan fluorescence in BSA is 10^{-9} s [11]. The k_q value was thus calculated to be of the order of $10^{15}\ M^{-1}\ s^{-1}$. The k_q depends on the probability of a collision between fluorophore and quencher and it is a measurement of exposure of tryptophan residues to drugs. This probability depends on their rate of diffusion (D), their size and concentration as shown in the following equation:

$$k_q = 4\pi a D\, Na \times 10^{-3} \tag{4}$$

where D is the sum of diffusion coefficients of quencher and fluorophore, a the sum of molecular radii and Na is the Avogadro's number. Upper limit of k_q expected as a diffusion-controlled bimolecular process is $10^{10}\ M^{-1}\ s^{-1}$ [16]. High magnitude of k_q observed here ($10^{15}\ M^{-1}\ s^{-1}$) can only occur by the process of energy transfer, indicating that the quenching of BSA fluorescence by RB is through intermolecular interaction forces [9].

3.2. Analysis of binding equilibria

Fluorescence intensity data can also be used to obtain the binding constant (K_a) and the number of binding sites (n). Equilibrium between free and bound molecules is given by Eq. (5) providing that small molecules bind independently to a set of equivalent sites on a macromolecule [16,17]:

$$\log\frac{(F_0 - F)}{F} = \log\ K_a + n\ \log[Q] \tag{5}$$

where K_a is the binding constant or the apparent association constant for drug–protein interaction, and n is the number of binding sites. Values of K_a and n can thereby be determined from the intercept and slope by plotting $\log(F_0 - F)/F$ versus $\log[Q]$. As can be seen in Table 2, the value of K_a as obtained is of the order of 10^5, which indicates that there is a strong interaction between RB and BSA. Value of n is approximately equal to 1, indicating that there is one class of binding site for RB towards BSA.

Table 1
Static and collisional quenching constants for RB–BSA system at different temperatures

T (K)	V ($\times 10^6\ M^{-1}$)	K_{sv} ($\times 10^6\ M^{-1}$)	R^2
298	3.18	2.63	0.9979
304	2.95	1.95	0.9938
310	1.99	1.83	0.9973

$C_{BSA} = 10\ \mu M$, $\lambda_{ex} = 295$ nm.

Table 2
Apparent binding constants K_a and binding sites n of the interaction of RB with BSA at different temperatures

T (K)	K_a ($\times 10^5\ M^{-1}$)	n	R^2
298	10.8	1.23	0.9961
304	5.43	1.19	0.9929
310	3.14	1.17	0.9973

$C_{BSA} = 10\ \mu M$, $\lambda_{ex} = 295$ nm.

3.3. Interacting forces between BSA and RB

Thermodynamic parameters relying on temperatures were analyzed to characterize the acting forces between drug and BSA. Basically, four types of interactions play vital roles in protein–drug binding, that is, hydrogen bonds, van der Waals forces, electrostatic forces, and hydrophobic interactions. Thermodynamic parameters, free energy changes (ΔG°) enthalpy changes (ΔH°) and entropy changes (ΔS°) of interactions are essential to interpret the binding mode. For the purpose of clarifying interaction of RB with BSA, the temperature dependence of binding constant was resulted from binding studies carried out at three different temperatures: 298, 304 and 310 K. When enthalpy change (ΔH°) does not vary significantly in the temperature range studied, both enthalpy change (ΔH°) and entropy change (ΔS°) can be determined from van't Hoff equation:

$$\ln K = -\frac{\Delta H^\circ}{RT} + \frac{\Delta S^\circ}{R} \tag{6}$$

In Eq. (6), K corresponds to the binding constant at specific temperature and R is the gas constant. ΔH° and ΔS° can be calculated from slopes and ordinates of the van't Hoff relationship. ΔG° was consequently obtained according to the following equation:

$$\Delta G^\circ = \Delta H^\circ - T\Delta S^\circ \tag{7}$$

Values of ΔG°, ΔH°, and ΔS° are summarized and listed in Table 3.

As can be seen in Table 3, the negative values of ΔG° and ΔH° along with the positive values of ΔS° are obtained for the RB–BSA interaction. Negative values of ΔG° reveal that the binding process is spontaneous. Positive values of ΔS° are evidence of hydrophobic interactions [18]. Moreover, a positive value of ΔS° along with a negative ΔH° value is characteristic of electrostatic interactions in aqueous solution. Thus, it is more likely that hydrophobic and electrostatic interactions are involved in binding process. Nevertheless, it is less possible that RB interacting with albumin through electrostatic interactions under our experimental conditions. Consequently, hydrophobic interaction plays a major role in the binding of RB with albumin.

3.4. Binding studies in the presence of ANS

It is known that ANS quenches the intrinsic fluorescence of BSA through hydrophobic and electrostatic interactions, and on the other hand, the fluorescence of ANS itself increases due to transfer of ANS from an aqueous to non-polar environment as a result of hydrophobic interactions with BSA [19,20]. Therefore, ANS can be used as a fluorescence probe to understand the interaction of RB with BSA.

Table 3
Apparent binding constants K_a and thermodynamic parameters of RB–BSA interaction

T (K)	K_a ($\times 10^5$ M^{-1})	ΔG° (kJ mol^{-1})	ΔH° (kJ mol^{-1})	ΔS° (J mol^{-1} K^{-1})
298	10.8	−35.90	−5.14	120.44
304	5.43	−36.62		
310	3.14	−37.34		

Fluorescence spectra of BSA upon addition of ANS/RB were first recorded upon excitation at wavelength of 295 nm. Fraction of bound (θ) was then determined according to equation as follows [21]:

$$\theta = \frac{F_0 - F}{F_0} \tag{8}$$

The value of θ for ANS bound to BSA was calculated to be 82%. While for RB bound to BSA, the value of θ was around 53% under the same conditions. This indicated that the interaction of ANS with BSA was stronger than that of RB with BSA.

Additionally, ANS–BSA interaction upon sequentially addition of RB was studied by recording fluorescence spectra of ANS in range of 390–550 nm upon excitation at 370 nm. It was observed that fluorescence intensity of ANS exhibited a slight decrease upon addition of RB. This is similar to the effect of rifampicin on the BSA–ANS interaction [9]. Thus RB, like rifampicin, may compete with ANS for binding to hydrophobic sites on the albumin surface.

3.5. Energy transfer between rifabutin and BSA

Föster's theory of non-radiative energy transfer was used as determining the distances between the BSA residue and RB bound to BSA. According to the Föster's theory, the energy transfer effect is not only related to the distance between the donor (tryptophan residue) and acceptor (RB), but also influenced by the critical energy transfer distance R_0, that is:

$$E = 1 - \frac{F}{F_0} = \frac{R_0^6}{R_0^6 + r^6} \tag{9}$$

where r is the distance between the acceptor and the donor, and R_0 is the critical energy transfer distance, at which 50% of the excitation energy is transferred to the acceptor is defined by the following equation:

$$R_0^6 = 8.8 \times 10^{-25} k^2 N^{-4} \Phi J \tag{10}$$

In Eq. (10), k^2 is the orientation factor related to the geometry of the donor–acceptor of dipole, N the refractive index of medium, and Φ is the fluorescence quantum yield of the donor. Spectra overlap integral J between the donor emission spectrum and the acceptor absorbance spectrum is then calculated by the equation:

$$J = \frac{\sum F(\lambda)\varepsilon(\lambda)\lambda^4 \Delta\lambda}{\sum \Sigma F(\lambda)\Delta\lambda} \tag{11}$$

where $F(\lambda)$ is the fluorescence intensity of fluorescence donor at wavelength of and $\varepsilon(\lambda)$ is molar absorbance coefficient of the acceptor when wavelength is λ. Under experimental conditions, it had been noted that $k^2 = 2/3$, $N = 1.336$ and $\Phi = 0.15$ for BSA [22].

The spectral overlap of UV absorption spectrum of RB and fluorescence emission spectrum of BSA is illustrated in

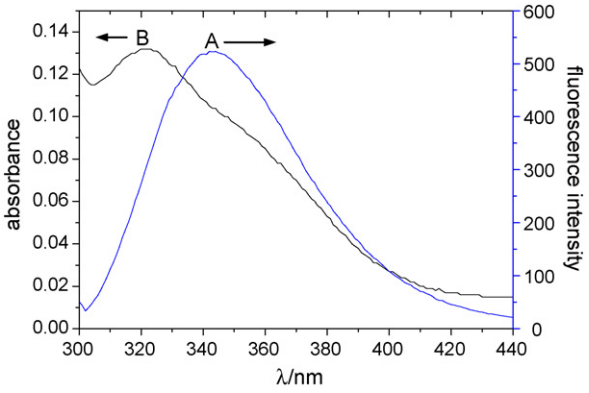

Fig. 3. Spectral overlap between (A) BSA fluorescence spectrum and (B) RB absorbance spectrum. $C_{BSA} = 10\,\mu M$, $C_{RB} = 10\,\mu M$.

Table 4
Binding constants K_a of RB–BSA complex in the presence of various metal ions at 298 K

	K_a ($\times 10^5\ M^{-1}$)	R^2
BSA–RB	10.8	0.9961
BSA–RB–Cu^{2+}	15.5	0.9916
BSA–RB–Zn^{2+}	8.12	0.9909
BSA–RB–Mg^{2+}	10.1	0.9952
BSA–RB–Ca^{2+}	15.3	0.9924

$C_{BSA} = 10\,\mu M$.

Fig. 3. It was then calculated that $J = 1.29 \times 10^{-14}\ cm^3\ L\ mol^{-1}$, $R_0 = 2.63$ nm, $E = 0.422$, and $r = 2.77$ nm. As the distance of donor to acceptor for RB–BSA binding is in the 2–8 nm scale [23], the energy transfer from BSA to RB occurs with high probability.

3.6. Influences of common ions on binding constant

Metal ions, especially those of bivalent type, are vital to human body and playing an essentially structural role in many proteins based on coordinate bonds. The presence of metal ions in plasma may affect interaction of drugs with BSA.

Effects of common bivalent metal ions (e.g. Cu^{2+}, Zn^{2+}, $Mg^{2+}$and Ca^{2+}) on binding constants of RB–BSA complex were investigated at 298 K. The values of binding constant K_a acquired in the present of metal ions are listed in Table 4.

It can be seen from Table 4 that the presence of Cu^{2+}, Ca^{2+} ions increases the binding constant of RB–BSA complex, whereas, the binding constant between RB and BSA decreases to various degrees in the presence of Zn^{2+} and Mg^{2+}. The higher binding constant possibly results from the formation of metal ion–RB complexes via metal ion bridge [24]. This may prolong storage period of RB in blood plasma and enhance its maximum effects. On the contrary, the decrease in binding constant may due to the formation of metal ion–BSA complexes. The formation of metal ion–albumin complexes is likely to affect conformation of protein, which may influence RB binding kinetics and even inhibit RB–BSA binding.

3.7. Conformational investigations

Influences of RB on the conformational changes of BSA were assessed by synchronous fluorescence and CD. Synchronous fluorescence measurements provide information about the molecular microenvironment in the vicinity of the fluorophore functional groups. Synchronous fluorescence spectra were obtained by simultaneously scanning excitation and emission monochromators. As $\Delta\lambda$ between excitation wavelength and mission wavelength is 15 nm, synchronous fluorescence offers characteristics of tyrosine residues, while when $\Delta\lambda$ is 60 nm, it provides the characteristic information of tryptophan residues. Synchronous fluorescence spectra of BSA upon addition of RB gained at $\Delta\lambda = 15$ and 60 nm are shown in Fig. 4.

As shown in Fig. 4, fluorescence intensity of both tryptophan and tyrosine decreases and a notable red shift at maximum emission upon addition of RB is observed, which indicates that the conformation of protein is changed. It is likely due to that the hydrophobic amino acid structure surrounding tryptophan and tyrosine residues in BSA tends to collapse slightly and thus tryptophan and tyrosine residues are exposed more to the aqueous phase.

Further evidence of conformational changes of BSA upon addition of RB was provided by CD data. CD is a sensitive technique to monitor conformational changes in protein upon interaction with ligand. CD spectra of BSA with various concentrations of RB are shown in Fig. 5. It is apparently

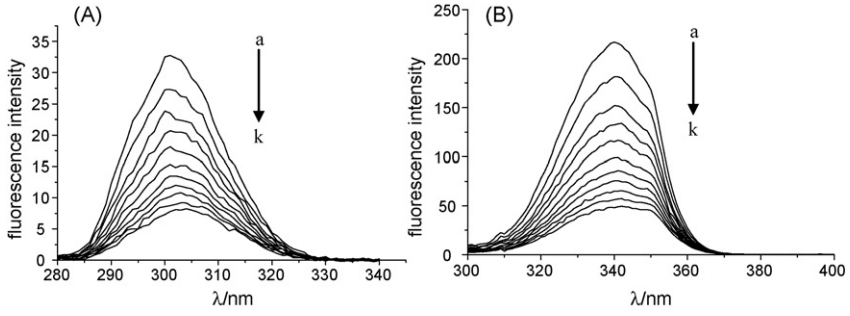

Fig. 4. Synchronous fluorescence spectra of BSA upon addition of RB at 298 K. (A) $\Delta\lambda = 15$ nm, (B) $\Delta\lambda = 60$ nm. $C_{BSA} = 10\,\mu M$; C_{RB} from (a) to (k): 0 μM (a), 2.25 μM (b), 4.5 μM (c), 6.75 μM (d), 9 μM (e), 11.25 μM (f), 13.5 μM (g), 15.75 μM (h), 18 μM (i), 20.25 μM (j) and 22.5 μM (k).

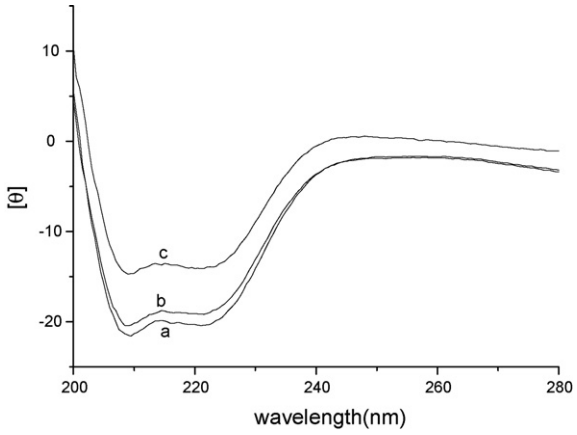

Fig. 5. CD spectra of BSA in the absence and presence of RB from 200 to 280 nm. (a) C_{BSA} = 1 μM, (b) C_{BSA} = 1 μM, C_{RB} = 1 μM, and (c) C_{BSA} = 1 μM, C_{RB} = 3 μM.

observed that CD spectral bands of BSA are at 208 and 222 nm, characteristic of a predominantly α-helical structure of BSA [25]. The addition of RB, however, led to a decrease in band intensity along all wavelengths of CD spectra without any significant shift of the peaks, indicating that RB changes the secondary structure of BSA. Moreover, the decrease in negative ellipticity means that the peptide strand extended even more, while the hydrophobicity was decreased. This conclusion agrees with the synchronous fluorescence result.

4. Conclusions

Interaction mechanism between RB and BSA was investigated by fluorescence spectroscopy and CD technique. The results show that RB is a strong quencher and interacts with BSA through a combination of dynamic and static quenching. The values of thermodynamic parameters ΔH°, ΔS° and ΔG° at different temperatures demonstrate that the binding reaction is mainly entropy-driven and hydrophobic interactions play a major role in the reaction. Synchronous spectra and CD data reveal that RB could change the conformation of BSA. Moreover, the presence of Cu^{2+} and Ca^{2+} increases the binding constants of RB–BSA complex, this may prolong storage period of RB in blood plasma and enhance its maximum effects.

Acknowledgements

We gratefully thank the financial support provided by Beijing Natural Science Foundation of China (no. 5073043), Scholastic Natural Science Foundation of Capital Medical University (no. 2005ZR06), and Beijing Municipal Project for Developing Advanced Human Resources for Higher Education.

References

[1] T. Peters, Biochemistry, Genetics and Medical Applications, Academic Press, San Diego, 1996.
[2] H.P. Rang, M.M. Dale, J. Ritter, Molecular Pharmacology, 3rd ed., Churchill Livingstone, New York, 1995.
[3] Y.J. Hu, Y. Liu, T.Q. Sun, A.M. Bai, H.Q. Lu, Z.B. Pi, Int. J. Biol. Macromol. 39 (2006) 280–285.
[4] S. Ashoka, J. Seetharamappa, P.B. Kandagal, S.M.T. Shaikh, J. Lumine. 121 (2006) 179–186.
[5] S.M.T. Shaikh, J. Seetharamappa, P.B. Kandagal, S. Ashoka, J. Mol. Struct. 786 (2006) 46–52.
[6] J. Rownicka, A. Sulkowska, J. Pozycka, B. Bojko, W.W. Sulkowski, J. Mol. Struct. 792 (2006) 243–248.
[7] Y.N. Shakina, V.V. Vostrikov, G.M. Sorokoumova, A.A. Selishcheva, V.I. Shvets, Bull. Exp. Biol. Med. 140 (2005) 711–713.
[8] N. Rastogi, K.S. Goh, M. Berchel, A. Bryskier, J. Antimicrob. Chemother. 46 (2000) 565–570.
[9] D.A. Mitchison, Int. J. Tuber. Lung Dis. 2 (1998) 612–615.
[10] B.P. Kamat, J. Seetharamappa, J. Chem. Sci. 117 (2005) 649–655.
[11] L.D. Ward, Methods Enzymol. 117 (1985) 400–414.
[12] H.M. Rawel, S.K. Frey, K. Meidtner, J. Kroll, F.J. Schweigert, Mol. Nutr. Food Res. 50 (2006) 705–713.
[13] J. Kang, Y. Liu, M.X. Xie, S. Li, M. Jiang, Y.D. Wang, Biochim. Biophys. Acta Genet. Subj. 1674 (2004) 205–214.
[14] M.R. Eftink, C.A. Ghiron, J. Phys. Chem. 80 (1976) 486–493.
[15] M.R. Eftink, C.A. Ghiron, Anal. Biochem. 114 (1981) 199–227.
[16] X.Z. Feng, Z. Lin, L.J. Yang, C. Wang, C.L. Bai, Talanta 47 (1998) 1223–1229.
[17] H. Gao, L. Lei, J. Liu, Q. Kong, X. Chen, Z. Hu, J. Photochem. Photobiol. A Chem. 167 (2004) 213–221.
[18] P.D. Ross, S. Subramanian, Biochemistry 20 (1981) 3096–3102.
[19] M. Moller, A. Denicola, Biochem. Mol. Biol. Educ. 30 (2002) 309–312.
[20] B. Klajnert, L. Stanislawska, M. Bryszewska, B. Palecz, Biochim. Biophys. Acta Proteins Proteomics 1648 (2003) 115–126.
[21] G. Weber, L.B. Young, J. Biol. Chem. 239 (1964) 1415–1419.
[22] B. Valeur, J.C. Brochon, New Trends in Fluorescence Spectroscopy, 6th ed., Springer Press, Berlin, 1999.
[23] Y.J. Hu, Y. Liu, J.B. Wang, X.H. Xiao, S.S. Qu, J. Pharm. Biomed. Anal. 36 (2004) 915–919.
[24] X.F. Liu, Y.M. Xia, Y. Fang, J. Inorg. Biochem. 99 (2005) 1449–1457.
[25] Y.J. Hu, Y. Liu, X.S. Shen, X.Y. Fang, S.S. Qu, J. Mol. Struct. 738 (2005) 143–147.